

Contrast and Clustering: Learning Neighborhood Pair Representation for Source-free Domain Adaptation

Yuqi Chen^a, Xiangbin Zhu^a, Yonggang Li^{b,*}, Yingjian Li^a and Haojie Fang^c

^a*School of Computer Science and Technology, Zhejiang Normal University, Jinhua, 321004, China*

^b*College of Information Science and Engineering, Jiaxing University, Jiaxing, 314001, China*

^c*School of Computer Science and Technology, Zhejiang Sci-Tech University, Hangzhou, 310018, China*

ARTICLE INFO

Keywords:

Source-free domain adaptation
Unsupervised domain adaptation
Contrastive learning
Transfer learning
Image classification

ABSTRACT

Unsupervised domain adaptation uses source data from different distributions to solve the problem of classifying data from unlabeled target domains. However, conventional methods require access to source data, which often raise concerns about data privacy. In this paper, we consider a more practical but challenging setting where the source domain data is unavailable and the target domain data is unlabeled. Specifically, we address the domain discrepancy problem from the perspective of contrastive learning. The key idea of our work is to learn a domain-invariant feature by 1) performing clustering directly in the original feature space with nearest neighbors; 2) constructing truly hard negative pairs by extended neighbors without introducing additional computational complexity; and 3) combining noise-contrastive estimation theory to gain computational advantage. We conduct careful ablation studies and extensive experiments on three common benchmarks: VisDA, Office-Home, and Office-31. The results demonstrate the superiority of our methods compared with other state-of-the-art works.

1. Introduction

The appetite for massive labeled training data has been successfully addressed in unsupervised learning. However, significant degradation will occur if the data distributions in the source and target domains are very different, which is formally denoted as domain/distribution shift. To tackle the generalization of the model to unseen domains, domain adaptation (DA) methods [1, 2] based on cotraining of source and target data are conceptually simple, i.e., transferring learned knowledge from the source domain to the target domain.

 202025201103@zjnu.edu.cn (Y. Chen); zhuxb@zjnu.edu.cn (X. Zhu); liyonggang@zjxu.edu.cn (Y. Li); liyingjian@zjnu.edu.cn (Y. Li); 18868901971@163.com (H. Fang)
ORCID(s): 0000-0001-9769-1167 (Y. Chen); 0000-0001-7281-6680 (X. Zhu); 0000-0002-7269-0368 (Y. Li)

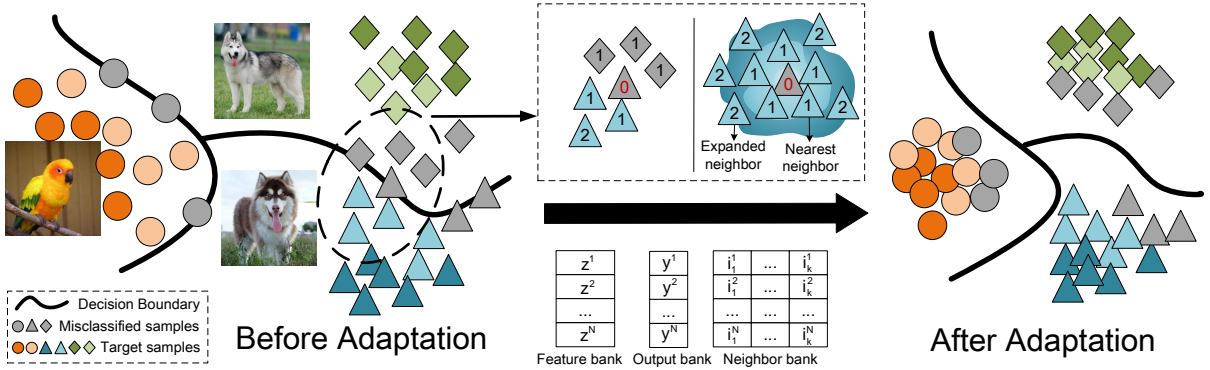


Figure 1: An overview of the proposed method. CaC learns features of the unlabeled target data from pretrained source network, and then these prototype features are used for unsupervised learning clustering.

However, with increasing concern about data privacy and data transfer bottlenecks of large datasets, it is extremely unrealistic to require the coexistence of source and target data. In this privacy-preserving scenario, previous unsupervised DA methods could not be deployed, and thus, source-free domain adaptation (SFDA) has emerged over time. The purpose of SFDA is to obtain high performance in an unlabeled target domain, where the source data are unavailable during the target adaptation process. Existing SFDA methods [3, 4, 5] try to better learn domain invariant/variant representations. However, the existing SFDA methods either require an auxiliary network[6, 7], or complex extra data processing is used[8, 9]. Other methods [10, 11] are negatively affected by noisy labels may predict incorrect target pseudolabels.

The above observation motivates us to tackle the data shift issue in SFDA. There are two obstacles: one is the unlabeled target data, and the other is that the source data cannot be obtained directly, relying only on the pretrained source model. Based on the fact that classes are shared between the source and target domains under the closed set setting[12, 13], it is reasonable to assume that the pretrained source model can learn the class representation of the target data. Therefore, even if the source and target data are shifted in the feature space, the features extracted by the source model on the target data can form rough clusters through intrinsic class representation information (e.g., husky should never be classified as parrot), where the softmax output of similar features should be highly consistent. To achieve domain adaptation without the need for specialized source training or changing the model structure, we expect to use the knowledge learned from the source model for self-supervised learning on unlabeled target data. Inspired by recent contrastive learning[14, 15] (which, as the name implies, learns feature representations by comparing positive and negative samples), it is shown that the data itself provide supervision for network learning. Unlike previous methods that only added samples or changed the definition of positive pairs, we first define two probability functions which represent the probability that a sample has the same category as its positive and negative samples, respectively. The

negative logarithm of these two probability functions is set as the objective function. Then, we propose a contrast and clustering (**CaC**) method. Specifically, we meticulously design positive and negative samples, then use extended neighbors to find hard samples, and finally, approximate the objective function with the noise-contrastive estimation theory. As illustrated in Figure 1, we define the nearest neighbor samples as positive pairs and the neighbors of other samples as negative pairs to achieve contrastive clustering with more sample pairs. Simultaneously, considering that harder negative pairs[16, 17] facilitate better and faster learning, we introduce extended neighbors to exclude similar samples from the negative pool to extract more valuable negative pairs. These extended neighbors are computationally costless because they are obtained by querying the nearest neighbor index in the memory bank. However, in practice, negative pair term is not always effective. We find that the contrastive self-supervised performance degrades on the class-imbalanced dataset, and we address this problem by recursively decoupling positive and negative samples[18] during training. The experimental results show that the proposed method is sufficiently effective on three source-free domain adaptation benchmarks.

The primary contributions of this work are as follows:

1. We propose a contrastive clustering method for source-free domain adaptation, which uses nearest neighbors to learn domain-invariant class features in an unsupervised manner, to achieve intra-class compactness and inter-class separation.
2. Extended neighbors are taken into account to mine more valuable negative pairs, and these extended neighbors are obtained by querying the nearest neighbor indexes in the memory bank without incurring additional computational cost.
3. The experimental results on three datasets demonstrate the effectiveness and achieve the state-of-the-art results.

2. Related Work

2.1. Domain Adaptation

Domain adaptation(DA) attempts to bridge the distribution gap between two domains to maximize the performance on target domain. There are four typical settings: close-set[19], open-set[20], partial-set[21], and universal[12]. Among them, close-set DA is the most commonly DA setting in which the number of categories in the source and target domains is identical. Conventional close-set DA methods assume that the categories are fully shared between the source and target domains. With this assumption, a number of DA methods based on learning invariant representations have been proposed to align distributions, which can be classified into three categories: domain-level alignment methods[22], class-level alignment methods[23] and both domain- and class-level alignment methods[24].

To generate similar feature distributions from different domain data, the early adversarial adaptation method [25] combines domain adaptation with a two-player game similar to generative adversarial networks(GAN). CDAN[26]

extends the conditional adversarial mechanism to enable discriminative and transferable domain adaptation. However, these GAN-based methods[27, 28] require auxiliary network. Without additional generative network, other methods obtain domain invariant features to minimize the domain discrepancy by conditional entropy minimization[29, 30, 31] or clustering loss[1, 32, 33]. McDalNets[30] formulates a new adaptation bound for DA based on the induced MCSD divergence as a measure of domain distance. CaCo[1] introduces contrastive learning, encouraging networks to learn representations with different categories but different domains. SRDC[32] directly reveals intrinsic target discrimination by discriminative clustering of target data. However, the source data are not directly available in practice due to privacy issues, making these methods inapplicable.

2.2. Source-Free Domain Adaptation

The above-mentioned normal domain adaptation methods need to access source domain data during target adaptation. To address this challenging unsupervised DA setting with only a trained source model provided as supervision, many methods[34, 35, 36, 37] have emerged to tackle source-free domain adaptation(SFDA), which has no way of accessing source data. According to application scenario, SFDA can be divided into three categories: single source to single target[38, 7], single source to multiple target[39] and multiple source to single target[9, 40]. Undoubtedly, the shortage of training data may increase the difficulty of model adaptation. To solve this problem, existing studies[38, 6, 19, 5, 3, 11] have pay more attention to single source to single target. SHOT[38] tunes the source classifier to encourage interclass feature clustering by maximizing mutual information and pseudolabeling. 3C-GAN[6] is based on conditional GAN to provide supervised adaptation by regularizing the source domain information gradually. NRC[19] proposes neighborhood clustering, which performs predictive consistency among local neighborhoods. CPGA[5] proposes a contrastive prototype generation strategy to generate feature prototypes for each class. U-SFAN[3] accounts for uncertainty by placing priors on the parameters of the source model. DIPE[11] captures such domain-invariant parameters in the source model to generate domain-invariant representations. However, these methods indirectly learn domain invariant features by generating features, such as GAN[6], generate strategy[5] or parameter update strategy[11], which is quite costly.

This paper is also focus on tackling the problem of single source to single target. Compared to existing SFDA work, the key difference in our work compared to existing SFDA work is that CaC maximizes the intra-class distance reduction and inter-class distance increase using neighborhood samples. NRC[19] is also based on the nearest neighbor clustering method, which needs to compute neighbors twice. By contrast, our CaC only needs to compute neighbors once and generate extended neighbors through the memory bank without introducing additional computation.

2.3. Contrastive Learning

Contrastive learning(CL) is a type of self-supervised learning that maximizes the distance between different categories and minimizes the distance between the same categories. As one of the classical methods, InfoNCE[15] is based on the principle of noise-contrast estimation[41] and converts data distribution solving into a multi-classification problem by constructing positive and negative sample pairs. There are various ways to construct positive and negative sample pairs. InvaSpread[42] and SimCLR[43] construct pair samples from the current mini-batch, where the augmented samples are positive pair. CMC[44] treats data from different views of the same scene as positive pairs and data from different scenes as negative pairs. NNCLR[45] uses data augmentation and its nearest neighbors in the memory bank as positive sample pairs. DCL[18] removes positive sample pairs from the denominator in contrast loss to achieve positive and negative term decoupling.

In domain adaptation, CL has been used for alignment of instances to address domains discrepancy[46, 47, 48, 49, 50]. CAN[46, 51] modifies Maximum Mean Discrepancy (MMD)[52] loss to be used as a contrastive loss. SwAV[47] proposes a contrastive pre-training method for UDA. CLDA[48] employs contrastive learning to form stable and correct cluster cores in the target domain. HCL[50] investigates memory-based learning for unsupervised source-free domain adaptation that learns discriminative representations for target data. However, all the above CL-based methods treat only the augmented instance of the same input as positive pair, and the rest of data or the random augmented data in current batch-size as negative pairs.

Compared with the above methods, our work has the advantage of setting the nearest multiple neighbors as positive pairs, which allows clustering directly in the original feature space without the use of augmentation techniques. More importantly, different from other neighbor-based contrastive learning methods[45, 53], we remove false negative pairs to prevent class clustering from collapsing. Even though CDA[49] takes this into account, it is accomplished by computing and sorting similarities, whereas our CaC is achieved by expanded neighbors without additional computation. Additionally, CDA removes only the exact same number of negative pairs in a mini-batch. To be specific, CDA removes 512 potential false negatives from all anchor images in a mini-batch, while our CaC adjusts the exclusion number according to the similarity of the samples within the current mini-batch.

3. Method

3.1. Problem Definition

Given the model \mathcal{M}_s trained on the labeled source domain $\mathcal{D}_s = \left\{ x_{s_i}, y_{s_i} \right\}_{i=1}^m$ and the unlabeled target domain $\mathcal{D}_t = \left\{ x_{t_i} \right\}_{i=1}^n$, assume the feature space $\mathcal{X}_s = \mathcal{X}_t$, label space $\mathcal{Y}_s = \mathcal{Y}_t$, but marginal probability $P_s(x_s) \neq P_t(x_t)$ with conditional probability $Q(y_s | x_s) \neq Q(y_t | x_s)$. The target domain and source domain have the same C categories in this paper (known as the closed-set problem). Our method splits the model \mathcal{M}_s into two parts: a feature

Table 1

Symbols and corresponding definitions.

Symbols	Definitions	Symbols	Definitions
D_s, D_t	The source and target domains	S	The size of mini-batch
x_{s_i}, x_{t_i}	The source and target data	C	The number of the class
m, n	The number of source and target data	d	The size of feature dimension
x_i	The i -th data in target domain	$z(x_i)$	Softmax output of data x_i
K	The number of nearest neighbors	f	Feature extractor network
\mathcal{K}	Nearest neighbors/positive pairs set of data x_i	\mathcal{C}	Classifier network
\mathcal{O}	Dissimilar samples/negative pairs set of data x_i	\mathcal{T}	Current mini-batch
\mathcal{B}	Current mini-batch data excluding data x_i	$M(\cdot)$	Similarity measurement

extractor f , and a classifier $C = f(x)^T W + b$. Therefore, the output of the model is denoted as $z(x) = \delta(C(f(x)))$, where δ denotes the softmax function. Specifically, we list all symbols in this paper and make brief explanations in Table 1.

The goal of source-free domain adaptation is to learn a feature extractor f and a classifier C to predict the labels $y_t \in Y_t$ for x_t in the target domain D_t . The first obstacle is that the source data are not accessible, and the second is the tremendous discrepancy between these two domains.

3.2. InfoNCE Revisiting

InfoNCE is a loss function widely used for contrastive learning. It defines the augmented data of each sample as its positive sample, and the remaining data in current mini-batch as negative sample. This loss function is as follows:

$$\mathcal{L}^{\text{InfoNCE}} = \sum_{i=1}^n \log \frac{e^{z(x_i)^T z(\tilde{x}_i)/\tau}}{\sum_{b \in \mathcal{B}} e^{z(x_i)^T z(x_b)/\tau} + e^{z(x_i)^T z(\tilde{x}_i)/\tau}} \quad (1)$$

where \tilde{x} denotes the positive sample, x_b denotes the negative sample, and $\tau \in \mathcal{R}^+$ is a scalar temperature parameter.

3.3. Motivation

Similar samples (e.g., husky and alaskan malamute) should have similar predictions, while dissimilar samples (e.g., husky and parrot) should have different predictions. Unlike the previous methods that regard an augmented sample as a positive pair, we set the neighbor samples (the top- K similar samples in the feature embedding) as positive pairs. This allows us to perform clustering directly on the data without any generative techniques, and it allows us to consider a greater number of positive pairs. The samples in the k -nearest neighbor set (measured by cosine similarity or Euclidean distance) \mathcal{K} are chosen as the positive pairs of the instance x_i , and the other samples not in this set are chosen as the negative pairs. Based on this setting, InfoNCE could expand to contain multiple positive pairs, and the loss function \mathcal{L} can be defined as follows:

$$\mathcal{L} = - \sum_{i=1}^n \sum_{j \in \mathcal{K}} \log \frac{e^{z(x_i)^T z(x_j)}}{\sum_{b \in \mathcal{B} \cup b \neq j} e^{z(x_i)^T z(x_b)} + e^{z(x_i)^T z(x_j)}} \quad (2)$$

Intuitively, similar samples (e.g., husky and alaskan malamute) belong to different categories. However, the above loss function simply extends InfoNCE to multiple positive pairs, encouraging the network to classify samples with high similarity into the same category and samples with low similarity into different categories. When two categories have similar features, the samples are likely to be misclassified. To avoid incorrectly pulling closer to neighbors of different categories, the network needs to encourage neighbors of the same category to be closer together and neighbors of different categories to be more distant.

3.4. Proposed Method

Assuming that the target feature of the source pretrained feature extractor can form clusters[38, 11], we exploit this intrinsic ability of the pretrained model to perform SFDA by considering neighborhood information. Firstly, in C-class classification, the probability of x_i belonging to class C_1 is:

$$P(Y = C_1 | X = x_i) = \frac{e^{z(x_{ij})}}{\sum_{c=0}^{C-1} e^{z(x_{ic})}} \quad (3)$$

where $z(x_{ik}) = w_k^T f(x_i)$ and it can be interpreted as the probability that instance x_i belongs to class k.

Now, we consider the following conditions. Given a unlabeled data x_i , its k-nearest neighbor set is $\mathcal{K} = \{x_{i1}, x_{i2}, \dots, x_{ik} | M(f(x_{ih}), f(x_i)) > M(f(x_q), f(x_i)), q \neq i \cup q \neq i^h, h = 1, 2, \dots, k\}$, and the set \mathcal{O} denotes the other dissimilar samples in the mini-batch. The methods for finding \mathcal{K} and \mathcal{O} are described in detail in Sec.3.5 and Sec.3.6, respectively. Intuitively, x_i and the neighbor set \mathcal{K} should belong to the same class, which means that their outputs are highly consistent in terms of the probability of the class they belong to. With the definition of \mathcal{K} , we claim that the Proposition 1 holds:

Proposition 1 (Class consistency of positive pairs). $\forall x_j \in \mathcal{K}, \forall x_q \in \mathcal{D}_t \cup q \neq j \cup q \neq i, e^{z(x_i)^T z(x_{ji})} > e^{z(x_i)^T z(x_{qi})}$

According to the Proposition 1, the output of x_i and its k-nearest neighbor set \mathcal{K} should be more similar to the output of the k-nearest neighbor set \mathcal{O}^k of the remaining data in the current batch, which means that the one-hot outputs of the positive pairs are highly consistent, which we call the output consistency of the positive pairs.

Proposition 2 (Output consistency of positive pairs). $\forall x_j \in \mathcal{K}, \forall x_q \in \mathcal{D}_t \cup q \neq j \cup q \neq i, e^{z(x_i)^T z(x_{ji})} > e^{z(x_i)^T z(x_{qi})}$

Therefore, we define two likelihood functions $P_{i,j}^{same}$: the probability that x_i has the same category as its positive samples, and $P_{i,j}^{dis}$: the probability that x_i has the same category as the neighbors of the corresponding negative samples.

$$P_{i,j}^{same} = \prod_{x_j \in \mathcal{K}} \frac{e^{z(x_i)^T z(x_j)}}{\sum_{q \neq i} e^{z(x_i)^T z(x_q)}} \quad (4)$$

$$P_{i,j}^{dis} = \prod_{x_j \in \mathcal{O}^k} \frac{e^{z(x_i)^T z(x_j)}}{\sum_{q \neq i} e^{z(x_i)^T z(x_q)}} \quad (5)$$

where \mathcal{O}^k denotes the corresponding k-nearest neighbors of \mathcal{O} . As the output consistency of neighbors is desired to be maximized, we propose to minimize the following negative logarithmic objective function and finally achieve clustering.

$$\begin{aligned} \mathcal{L} &= -\frac{1}{n} \sum_{i=1}^n \log \frac{P_{i,j}^{same}}{P_{i,j}^{dis}} \\ &= \frac{1}{n} \sum_{i=1}^n \left(\sum_{x_j \in \mathcal{O}^k} z(x_i)^T z(x_j) - \sum_{x_j \in \mathcal{K}} z(x_i)^T z(x_j) \right) + \\ &\quad \frac{1}{n} \sum_{i=1}^n (|\mathcal{K}|(1 - |\mathcal{O}|) \log \sum_{q \neq i} e^{z(x_i)^T z(x_q)}) \end{aligned} \quad (6)$$

Step 1 (upper bound): With the set $|\mathcal{O}| = |\mathcal{K}| \times |\mathcal{B}|$, then the constant term $|\mathcal{K}|(1 - |\mathcal{O}|) \leq 0$. Under the fact that the logarithm function is convex, combined with Jensen's inequality, we can obtain

$$\begin{aligned} \mathcal{L} &\leq \frac{1}{n} \sum_{i=1}^n \left(\sum_{j \in \mathcal{O}^k} z(x_i)^T z(x_j) - \sum_{j \in \mathcal{K}} z(x_i)^T z(x_j) \right) + \\ &\quad \frac{1}{n} \sum_{i=1}^n \left(\frac{N-1}{|\mathcal{K}|(1-|\mathcal{O}|)} \left(\sum_{q \neq i} z(x_i)^T z(x_q) + \log(N-1) \right) \right) \end{aligned} \quad (7)$$

Step 2 (approximation): In the real world, it is difficult to calculate the last term in the Eq.(7) due to the huge amount of data. Thanks to the success of noise-contrastive estimation theory[15, 41], we can simply approximate the entire dataset by negative samples. Then we can obtain

$$\begin{aligned} \mathcal{L} &\approx \frac{1}{n} \sum_{i=1}^n \left(\sum_{x_j \in \mathcal{O}^k} z(x_i)^T z(x_j) - \sum_{x_j \in \mathcal{K}} z(x_i)^T z(x_j) \right) + \\ &\quad \frac{1}{n} \sum_{i=1}^n \left(\frac{N-1}{|\mathcal{K}|(1-|\mathcal{O}|)} \left(\sum_{x_j \in \mathcal{O}^k} z(x_i)^T z(x_j) + \log(N-1) \right) \right) \end{aligned} \quad (8)$$

Finally, we omit the constant term in Eq.(8) and obtain

$$\mathcal{L}^{\text{CaC}} = \frac{1}{n} \sum_{i=1}^n \underbrace{\left(\sum_{x_j \in \mathcal{O}^k} z(x_i)^T z(x_j) \right)}_{\text{neg: negative pairs}} - \underbrace{\left(\sum_{x_j \in \mathcal{K}} z(x_i)^T z(x_j) \right)}_{\text{pos: positive pairs}} \quad (9)$$

The final function denoted as CaC, which is the approximation of the original objective function. Note that the

approximation is more accurate when more negative samples are used, which requires us to obtain more negative samples.

3.5. Finding the Nearest Neighbors

To retrieve the nearest neighbors for batch training, we build three memory banks: $\mathcal{F} \in \mathbb{R}^{n \times d}$ stores all target features, $\mathcal{P} \in \mathbb{R}^{n \times C}$ stores the corresponding prediction scores, and $\mathcal{N} \in \mathbb{R}^{n \times K}$ stores the corresponding top-K nearest data. For two memory banks, \mathcal{F} and \mathcal{P} , which are initialized to all target features and their predictions, only the features and their predictions computed in each small batch are used to update these two repositories, as in a previous study [10, 19].

For each data x_i , its nearest neighbors set, denoted as $\mathcal{K} = \text{topK}(f(x_i))$, are the samples with the top-K highest similarity to the memory bank \mathcal{F} , and are used to compute the positive pairs in Eq.(9). The cosine similarity is choice as the distance measurement in this work. The similarity between the two samples is at a maximum when the two softmax outputs have the same prediction class and are close to a one-hot vector.

3.6. Finding the Truly Negative Pair

The difference between our work and previous work is that we use extended neighbors to mine the truly informative negative samples. This step is efficient and does not require any additional computation, since the nearest neighbors are already computed in the positive pairs and the memory bank \mathcal{N} facilitates the retrieval of extended neighbors. More specifically, the memory bank \mathcal{N} is initialized to empty, and the indexes of the positive sample pairs for each sample are updated in the corresponding position during each training iteration. Since the nearest neighbor bank only stores the indexes of the neighbors, and each neighbor has a specific index which is the same in the dataset and the bank, it is convenient to obtain extended nearest neighbors.

For the negative pair term in Eq.(9), since other samples in the mini-batch may come from the same category as x_i , we claim that these similar samples should be excluded in the corresponding negative pair set \mathcal{O} , because these similar samples play a relatively unimportant part in the negative pair term. The selection of informative negative pairs turns out to be a hard task, especially in the absence of target labels. To find these similar samples, instead of simply using a larger K to find more neighbors or computing the nearest neighbors again[19], we utilize the expanded neighbors of each data, i.e., the nearest neighbors of each data and the nearest neighbors of these nearest neighbors. The data x_j is regarded as a similar sample of x_i if $x_j \in \text{topK}(\text{topK}(f(x_i)))$. Note that after we update the neighbor bank \mathcal{N} , $\text{topK}(\text{topK}(f(x_i)))$ can be easily retrieved in this bank. For each data in the current mini-batch, the weight $W_{sim} \in \mathbb{R}^{S \times S}$ is used to exclude those data that are similar in negative pair set, and non-zero elements are treated as negative pairs. Taking the data x_i as an example, if x_j is its similar sample, then the j-th column of the i-th row in W_{sim}

Algorithm 1 Learning Nearest Pair Representations for SFDA**Input:** Source-pretrained model \mathcal{M}_s , unlabeled target data \mathcal{D}_t .

- 1: Build three memory banks to store all the target features(\mathcal{F}) and predictions(\mathcal{P}) and the indexes of neighbors(\mathcal{N}).
- 2: Initialize the \mathcal{P} and \mathcal{F} banks by model \mathcal{M}_s .
- 3: **while** Adaptation **do**
- 4: Sample a mini-batch \mathcal{T} from \mathcal{D}_t and update memory banks \mathcal{P} and \mathcal{F} .
- 5: For each feature in \mathcal{T} , find its K-nearest neighbors \mathcal{K} and update memory bank \mathcal{N} .
- 6: Retrieve and expand the neighbors from memory bank \mathcal{N} to generate W_{sim}
- 7: Compute the loss function \mathcal{L}^{CaC}
- 8: Back-propagate with the loss function and update the network parameters
- 9: **end while**
- 10: **return** solution

is zero and the other positions are one. Finally, for each data x_i , its corresponding negative pair set is denoted as:

$$\mathcal{O} = \text{nondiag}(W_{sim})[:, i] \cdot \mathcal{B} \quad (10)$$

where $\text{nondiag}(W_{sim}) \in \mathbb{R}^{S-1 \times S}$ and $\text{nondiag}(\cdot)$ is the operation to obtain non-diagonal elements, and the set $\mathcal{B} \in \mathbb{R}^{(S-1) \times 1}$ denotes the remaining data in the current mini-batch.

And then retrieve the neighbors of \mathcal{O} from the memory bank \mathcal{N} , which is denoted as \mathcal{O}^k . As more negative samples are obtained by retrieving neighbors, it is better to approximate the whole dataset.

In summary, the two terms interact to achieve self-supervision of the features, where positive pairs are expected to improve the consistency of the one-hot outputs while negative pairs are expected to improve the diversity of the outputs. The weight W_{sim} is used to mine truly hard negative pairs. Our algorithm is illustrated in Algorithm 1.

4. Experiments

4.1. Datasets

We conduct the experiments on three benchmark datasets: **VisDA** is a more challenging dataset, with 12-class synthetic-to-real object recognition tasks. Its source domain consists of 152k synthetic images while the target domain contains 55k real object images. **Office-Home** contains 4 domains(Art, Clipart, Real World, Product) with 65 classes and a total of 15,500 images. **Office-31** contains 3 domains(Amazon, Webcam, DSLR) with 31 classes and 4652 images.

4.2. Evaluation

The column SF in the tables denotes source-free setting. For VisDA, we show accuracy for all classes and average over those classes (Avg in the tables). For Office-31 and Office-Home, we show the results of each task and the average accuracy over all tasks (Avg in the tables).

Table 2

Classification accuracy (%) on VisDA(Synthesis → Real) based on ResNet101.

Method	SF	VisDA												
		plane	bicycle	bus	car	horse	knife	mcycl	person	plant	sktbrd	train	truck	Avg
ResNet-101[54]	✗	55.1	53.3	61.9	59.1	80.6	17.9	79.7	31.2	81.0	26.5	73.5	8.5	52.4
DANN[25]	✗	81.9	77.7	82.8	44.3	81.2	29.5	65.1	28.6	51.9	54.6	82.8	7.8	57.4
CDAN[26]	✗	85.2	66.9	83.0	50.8	84.2	74.9	88.1	74.5	83.4	76.0	81.9	38.0	73.9
CaCo[1]	✗	90.4	80.7	78.8	57.0	88.9	87.0	81.3	79.4	88.7	88.1	86.8	63.9	80.9
SHOT[38]	✓	94.3	88.5	80.1	57.3	93.1	94.9	80.7	80.3	91.5	89.1	86.3	58.2	82.9
3C-GAN[6]	✓	94.8	73.4	68.8	74.8	93.1	95.4	88.6	84.7	89.1	84.7	83.5	48.1	81.6
NRC[19]	✓	96.8	91.3	82.4	62.4	96.2	95.9	86.1	80.6	94.8	94.1	90.4	59.7	85.9
CPGA[5]	✓	94.8	83.6	79.7	65.1	92.5	94.7	90.1	82.4	88.8	88.0	88.9	60.1	84.1
DIPE[11]	✓	95.2	87.6	78.8	55.9	93.9	95.0	84.1	81.7	92.1	88.9	85.4	58.0	83.1
U-SFAN+[3]	✓	94.9	87.4	78.0	56.4	93.8	95.1	80.5	79.9	90.1	90.1	85.3	60.4	82.7
CaC(Ours)	✓	96.9	91.0	83.3	72.3	96.9	96.1	90.7	81.6	95.1	92.9	92.0	63.2	87.7

Table 3

Classification accuracy (%) on Office-Home based on ResNet50.

Method	SF	Office-Home												Avg
		A→C	A→P	A→R	C→A	C→P	C→R	P→A	P→C	P→R	R→A	R→C	R→P	
ResNet-50[54]	✗	34.9	50.0	58.0	37.4	41.9	46.2	38.5	31.2	60.4	53.9	41.2	59.9	46.1
DANN[25]	✗	45.6	59.3	70.1	47.0	58.5	60.9	46.1	43.7	68.5	63.2	51.8	76.8	57.6
CDAN[26]	✗	50.7	70.6	76.0	57.6	70.0	70.0	57.4	50.9	77.3	70.9	56.7	81.6	65.8
SRDC[32]	✗	52.3	76.3	81.0	69.5	76.2	78.0	68.7	53.8	81.7	76.3	57.1	85.0	71.3
SHOT[38]	✓	57.1	78.1	81.5	68.0	78.2	78.1	67.4	54.9	82.2	73.3	58.8	84.3	71.8
NRC[19]	✓	57.7	80.3	82.0	68.1	79.8	78.6	65.3	56.4	83.0	71.0	58.6	85.6	72.2
U-SFAN+[3]	✓	57.8	77.8	81.6	67.9	77.3	79.2	67.2	54.7	81.2	73.3	60.3	83.9	71.9
CaC(Ours)	✓	59.0	79.5	82.0	67.6	79.2	79.5	66.7	56.5	81.3	74.2	58.3	84.7	72.4

4.3. Baselines

We compare CaC with three types of baselines: (1) source-only: ResNet[54]; (2) UDA with source data: DANN[25], CDAN[26], SRDC[32], CaCo[1]; and (3) source-free UDA: SHOT[38], 3C-GAN[6], NRC[19], CPGA[5], U-SFAN+[3], DIPE[11].

4.4. Implementation details.

To ensure fair comparison with related methods, we use the same network architecture as SHOT and adopt SGD with momentum 0.9 and batch size of 64 for all datasets. Specifically, we adopt the backbone of ResNet50 for Office-Home and Office31, and ResNet101 for VisDA. The learning rate for Office-Home and Office31 is set to 1e-3 for all layers, except for the last two newly added fc layers, where we apply 1e-2. Learning rates are set 10 times smaller for VisDA. We train 15 epochs for VisDA, 40 epochs for Office-Home and 100 epochs for Office-31. The code is available at <https://github.com/yukilulu/CaC>.

Table 4

Classification accuracy (%) on Office-31 based on ResNet50.

Method	SF	Office-31						
		A→D	A→W	D→A	D→W	W→A	W→D	Avg
ResNet-50[54]	✗	68.9	68.4	62.5	96.7	60.7	99.3	76.1
DANN[25]	✗	82.0	96.9	99.1	79.7	68.2	67.4	82.2
CDAN[26]	✗	92.9	94.1	71.0	98.6	69.3	100.0	87.7
CaCo[1]	✗	89.7	98.4	100.0	91.7	73.1	72.8	87.6
SHOT[38]	✓	94.0	90.1	74.7	98.4	74.3	99.9	88.6
3C-GAN[6]	✓	92.7	93.7	98.5	99.8	75.3	77.8	89.6
NRC [19]	✓	96.0	90.8	75.3	99.0	75.0	100.0	89.4
U-SFAN+ [3]	✓	94.2	92.8	74.6	98.0	74.4	99.0	88.8
CaC(Ours)	✓	95.2	93.8	74.7	99.1	76.3	99.8	89.9

Table 5

Classification accuracy(%) comparison with different components on VisDA

SHOT	\mathcal{L}_{CaC}	W_{sim}	Avg
✓			82.9
	✓		87.15
	✓	✓	87.7

4.5. Comparison with Other State-of-the-Art Methods

In this section, we compare our proposed CaC with the state-of-the-art methods on three DA benchmarks. In Table 2, Table3 and Table 4, the top part shows the results for the DA methods with access to source data during adaptation. The bottom shows the results for the SFDA methods. The best results are bolded, and the second-best results are underlined.

Specifically, CaC outperforms other SOTA methods on the more challenging dataset **VisDA**, achieving the best results in various categories and ultimately obtaining excellent results, as shown in Table 2. For **Office-Home**, the proposed CaC obtains better results compared with other SFDA methods, as shown in Table 3. Note that our method is superior in the tasks A→C, A→R, C→R and P→C. In addition, CaC obtains similar results to the SOTA in **Office-31**, as shown in Table 4. The main result is that VisDA provides sufficient data for learning positive and negative pairs so that CaC can learn better domain-invariant representations to achieve clustering of same-class samples. Moreover, CaC is able to outperform recent methods with source data (e.g., CaCo and SRDC), which demonstrates the superiority of our proposed method.

4.6. Analyzing and Ablating

4.6.1. Ablation study on the proposed \mathcal{L}_{CaC} and weight W_{sim}

To investigate the improvement bring by the two components, we show the quantitative results of the model optimized by different losses. As shown in Table 5, our proposed comparison and clustering loss \mathcal{L}_{CaC} achieves better results on VisDA than SHOT due to the pseudo-labeling that may give high confidence values for incorrect samples.

Contrast and Clustering

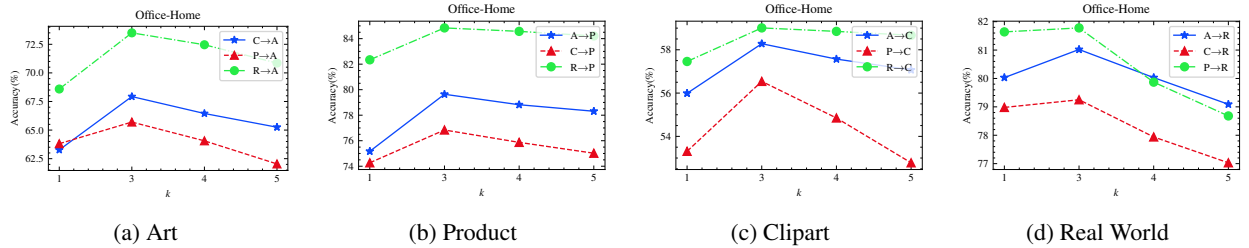


Figure 2: Classification accuracy(%) on Office-Home with different K values

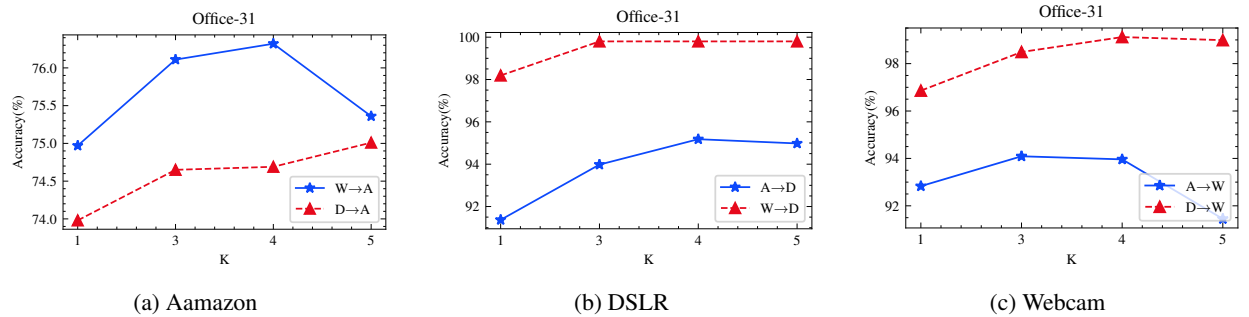


Figure 3: Classification accuracy(%) on Office-31 with different K values.

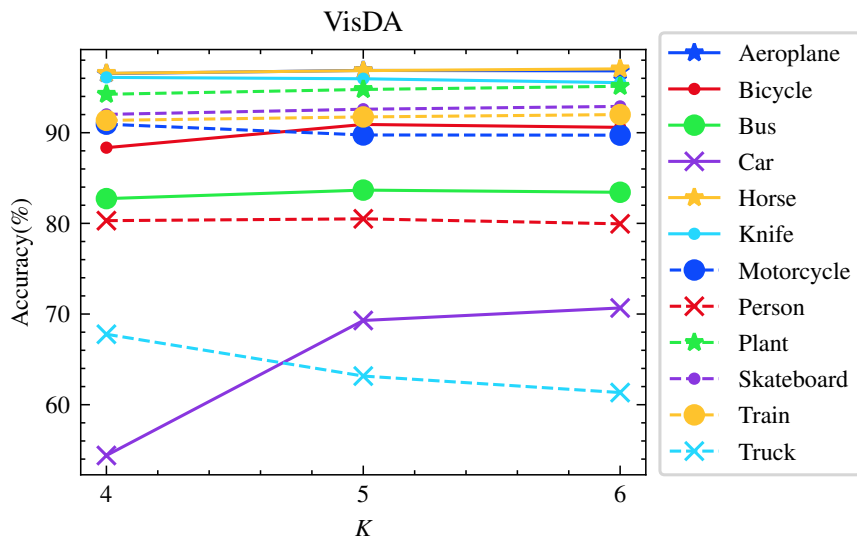


Figure 4: Classification accuracy(%) on VisDA with different K values.

Such results validate that neighbor pairs can give the network excellent self-supervised clustering ability. Moreover, we obtained the best performance when extracting more valuable negative sample pairs by using the weights W_{sim} generated from the nearest neighbors and extended neighbors.

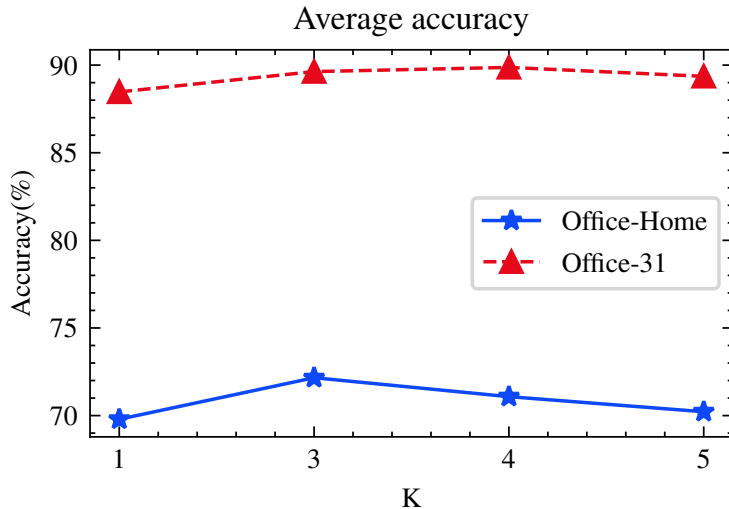


Figure 5: Average accuracy(%) on Office-Home and Office-31.

4.6.2. Number of neighbors K

For the number of neighbors K used for feature clustering in Eq.(9), we show the sensitivity of our method to the parameter K on each of the three datasets in Figure 2- Figure 4. From Eq.(9), we can see that K is correlated with the sample size of the dataset, requiring a larger value on the larger VisDA dataset and a relatively smaller value for Office-Home. Additionally, we show the average accuracy on Office-Home and Office-31 in Figure 5, where the smaller datasets Office-Home and Office-31 obtain higher accuracy when K is 3 or 4.

As can be summarized from the results, larger K values consider more pairs, which is better for learning a robust bound. However, setting too large a K value may also include samples from other categories, bringing more noisy samples, which leads to performance degradation.

4.6.3. Interesting impact of negative pairs

We find that CaC maintains the accuracy improvement on Office-Home, but degrades at a later stage on VisDA as shown in the green curve in Figure 6. We first consider the class comparison of these two datasets. As shown in Figure 7 and Figure 8, VisDA suffers from a worse class imbalance problem than Office-Home, which has a smaller number of classes and, even worse, a large gap in class proportions. Taking the fourth class of VisDA:car as an example, it is clear that a large proportion of the samples in a mini-batch belong to the car class, and the contrast loss treats the other samples in the mini-batch as potentially negative pairs. Ultimately, the network separates these samples that belong to the same class, resulting in a decrease in accuracy. As shown in Figure 8, CaC is much less accurate for classes with large quantities (car and truck) than other classes.

Observing that sampling negative examples with truly different labels improved performance in [55], we utilize

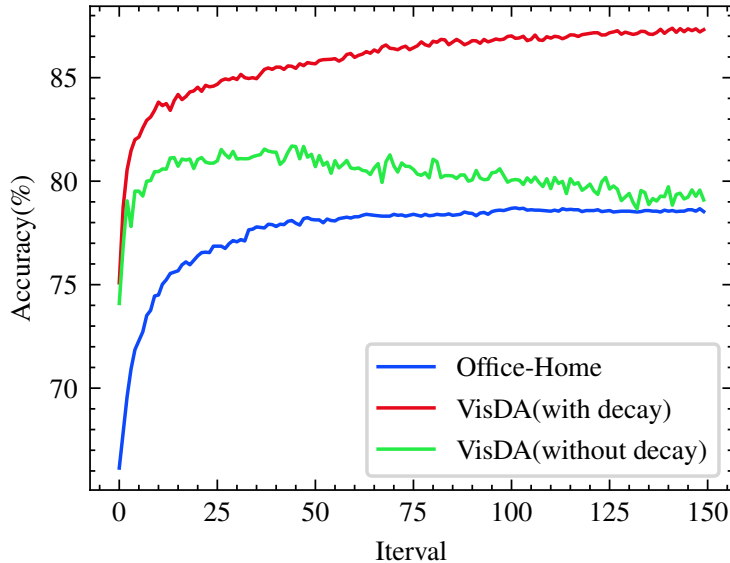


Figure 6: Classification accuracy(%) comparisons on the Office-Home and VisDA datasets. VisDA is set to with and without decay and Office-Home is only set to without decay for a clearer comparison.

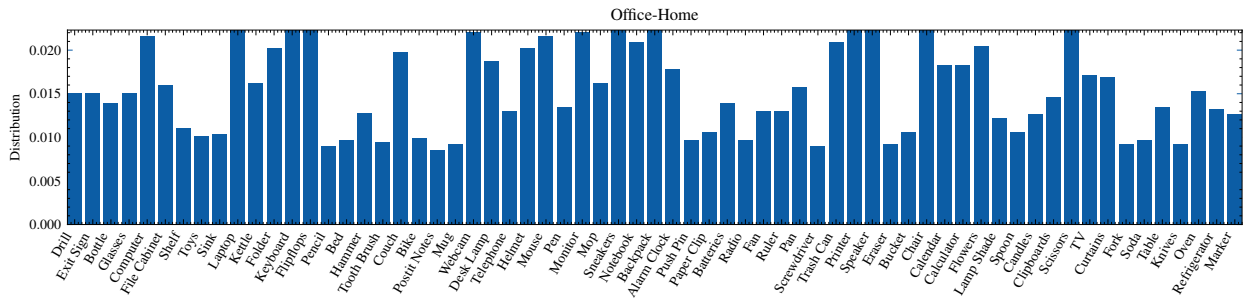


Figure 7: The class distribution on Office-Home.

extended nearest neighbors to find more valuable negative samples; however, negative pair term that pull apart the samples may dominate the loss values in the later training. Therefore, we introduce a factor $\alpha = (\frac{\text{max_iter}}{\text{max_iter} + \text{iter}})^\beta$ to control the impact of negative pairs. As the epoch time increases, the impact of the negative pairs will be reduced, where $\text{max_iter} = \text{batch size} \times \text{epoch}$ and β controls the rate of decrease; the larger its value is, the faster the negative pair impact decreases. The accuracy on VisDA can be steadily improved by introducing β . The comparison results with and without decay are shown in Figure 6. To further explore the effect of β on VisDA, we show the accuracy results for each category at different values in Figure 9. The accuracy can be steadily improved by introducing larger values. Specifically, we observe that as the β increases, the accuracy of the two most numerous categories, car and truck, improves significantly, while the other categories maintain high accuracy, which proves the effectiveness and robustness of the decay factor.

Also, we show the results on different value of β on the other two datasets. For Office-Home, we report the forth

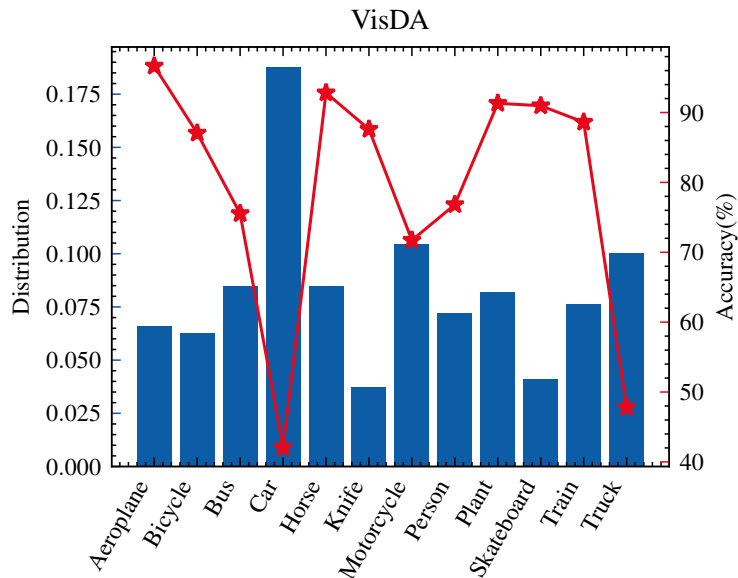


Figure 8: The distribution and the classification accuracy(%) of each class on VisDA.

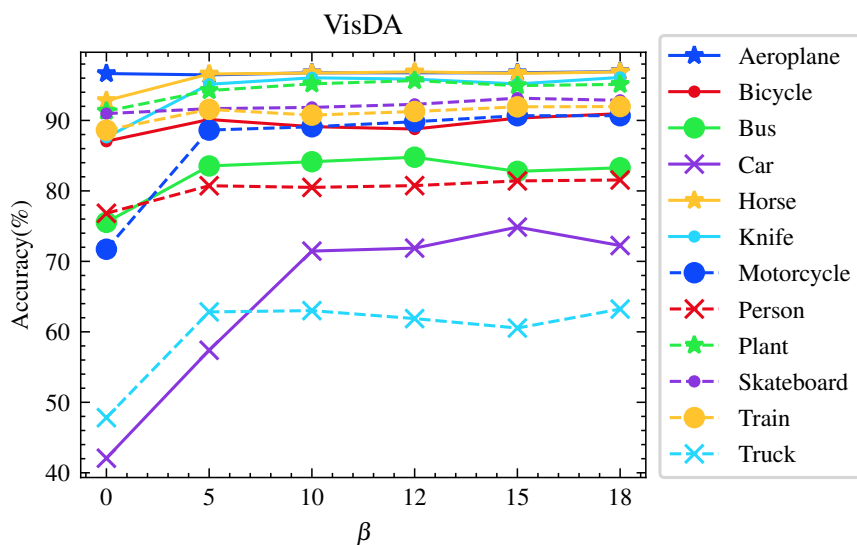


Figure 9: Classification accuracy(%) on VisDA with different β values

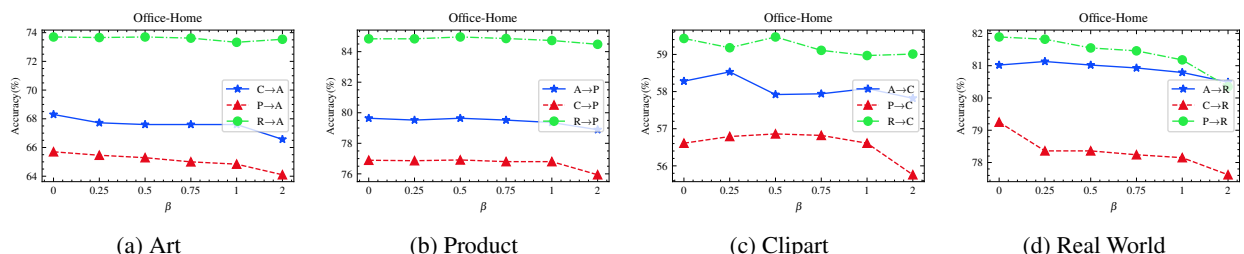


Figure 10: Classification accuracy(%) on Office-Home with different β values

Contrast and Clustering

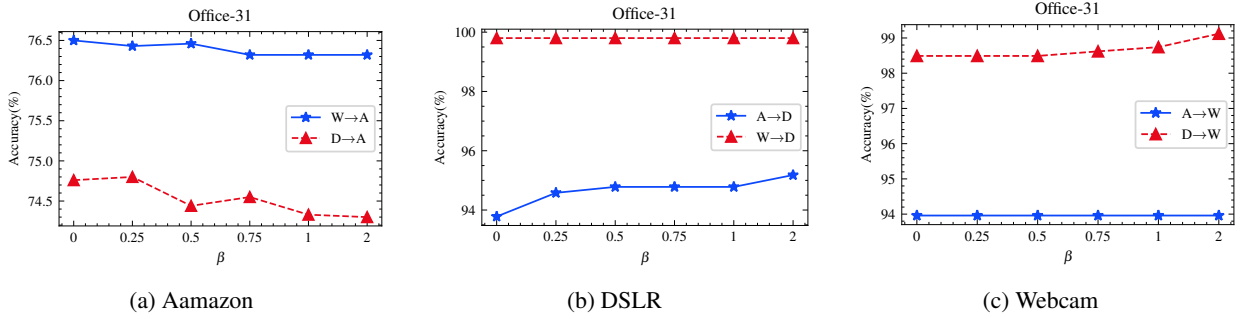


Figure 11: Classification accuracy(%) on Office-31 with different β values

Table 6

Runtime analysis and the average accuracy(%) of SHOT and our methods on VisDA. 30% denote the percentage of target features stored in the memory bank.

Method	Runtime(s/epoch)	Avg
SHOT	485	82.9
CaC(Ours)	471	87.7
30% for memory bank	466	87.5

domain as shown in Figure 10, we can observe that performance degradation is encountered in two domains, Clip and Real World. However, Office-Home maintains the relatively robust result with the increase of the β in Art and Product domains. For Office-31, it is not sensitive to the β value and maintains a high performance on different value.

4.6.4. Runtime analysis

We compare the runtime in one epoch with SHOT in Table 6. For SHOT, the pseudo-label is computed by clustering in each iteration. In contrast, our nearest neighbor samples are obtained by computing a dot product operation on the samples with the memory bank \mathcal{F} and then taking the top-K most similar samples. It is really simple because the dot product is equal to the cosine distance after feature normalization. Even though the weights W_{sim} need to use extended nearest neighbors, no additional computational consumption is required because these extended nearest neighbors can be directly retrieved from the neighbor bank \mathcal{N} . Therefore, our method can improve the performance with less computation. Additionally, we reduce the size of the repository, which does not incur significant performance loss and maintains competitive results.

4.6.5. Feature visualization

We visualize and analyze the learned features before and after adaptation for further validating the effectiveness of our method. The visualization of TSNE is performed on two datasets:Office-Home and VisDA. For the dataset Office-Home with a larger number of classes in the Figure 12, CaC achieves intra-class compactness and inter-class separation. Similarly, for the more challenging synthetic-to-real dataset VisDA in Figure 13, the classification boundaries are more obvious due to our contrast learning strategy.

5. Conclusion

In this paper, we propose a method for unsupervised domain adaptation without access to source data, which learns domain-invariant features by encouraging output consistency with nearest neighbors. Our method differs from previous methods in that we build an indexed memory bank for nearest neighbor samples to facilitate the retrieval of expanded neighbors, which are used to mine more valuable negative pairs without increasing the computational cost. Extensive experiments verify the importance of nearest neighbors and the impact of negative pairs as well as proving that the proposed method outperforms other state-of-the-art source-free domain adaptation methods on three benchmarks.

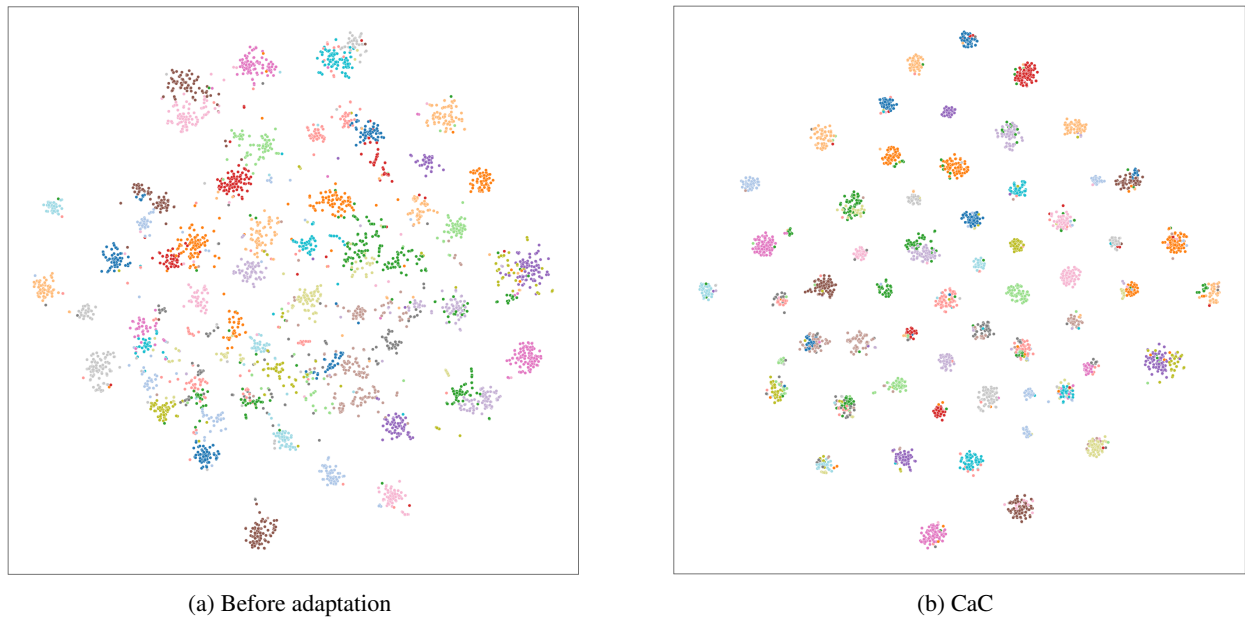


Figure 12: The TSNE visualization on Office-Home.

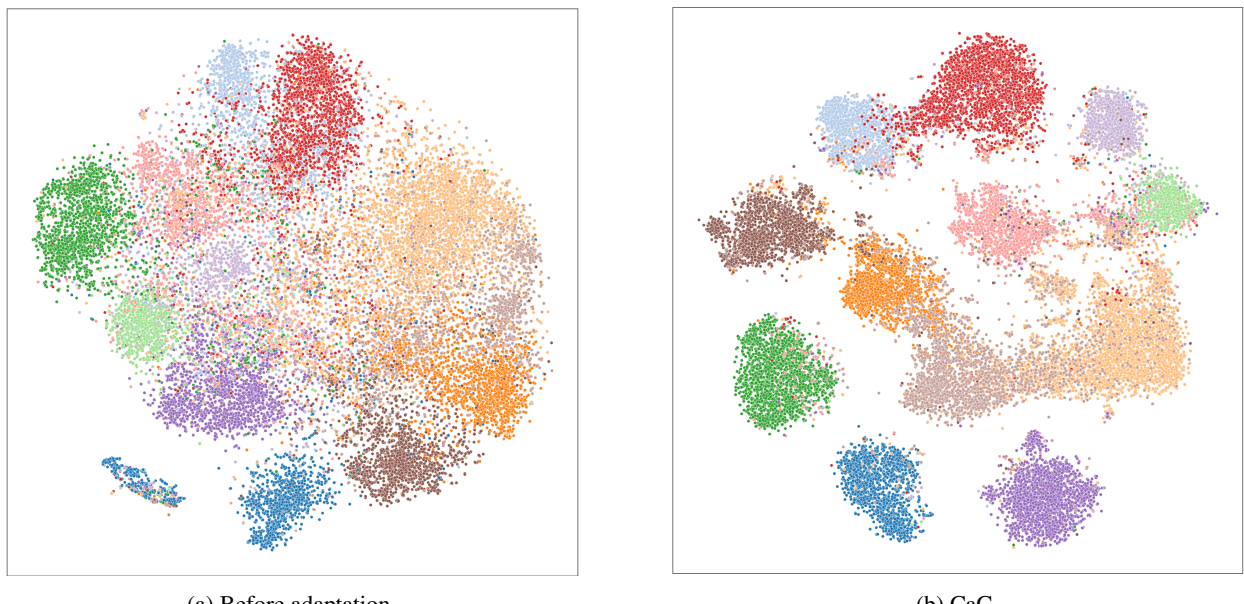


Figure 13: The TSNE visualization on VisDA.

CRediT authorship contribution statement

Yuqi Chen: Methodology, Data curation, Visualization, Investigation, Writing-original draft. **Xiangbin Zhu:** Supervision, Validation. **Yonggang Li:** Supervision, Writing-review&editing. **Yingjian Li:** Validation. **Haojie Fang:** Validation.

Declaration of competing interest

The authors declare that they have no known competing financial interests or personal relationships that could have appeared to influence the work reported in this paper.

Acknowledgement

This work was partially supported by the National Natural Science Foundation of China (NSFC Grant No. 61972059), Provincial Natural Science Foundation of Zhejiang (Grant No. LY19F020017), Jiaxing Science and Technology Project (Grant No.2022AD10017), Scientific Research Fund of Zhejiang Provincial Education Department (Grant No.Y202147449).

References

[1] J. Huang, D. Guan, A. Xiao, S. Lu, L. Shao, Category contrast for unsupervised domain adaptation in visual tasks, in: Proceedings of the IEEE/CVF Conference on Computer Vision and Pattern Recognition, 2022, pp. 1203–1214.

[2] K.-Y. Lin, J. Zhou, Y. Qiu, W.-S. Zheng, Adversarial partial domain adaptation by cycle inconsistency, in: European Conference on Computer Vision, Springer, 2022, pp. 530–548.

[3] S. Roy, M. Trapp, A. Pilzer, J. Kannala, N. Sebe, E. Ricci, A. Solin, Uncertainty-guided source-free domain adaptation, in: European Conference on Computer Vision, 2022, pp. 537–555.

[4] Y. Hou, L. Zheng, Visualizing adapted knowledge in domain transfer, in: Proceedings of the IEEE/CVF Conference on Computer Vision and Pattern Recognition, 2021, pp. 13824–13833.

[5] Z. Qiu, Y. Zhang, H. Lin, S. Niu, Y. Liu, Q. Du, M. Tan, Source-free domain adaptation via avatar prototype generation and adaptation, in: Proceedings of the Thirtieth International Joint Conference on Artificial Intelligence, Montreal, Canada, 2021, pp. 2921–2927.

[6] R. Li, Q. Jiao, W. Cao, H.-S. Wong, S. Wu, Model adaptation: Unsupervised domain adaptation without source data, in: Proceedings of the IEEE/CVF Conference on Computer Vision and Pattern Recognition, 2020, pp. 9641–9650.

[7] H. Xia, H. Zhao, Z. Ding, Adaptive adversarial network for source-free domain adaptation, in: Proceedings of the IEEE/CVF International Conference on Computer Vision, 2021, pp. 9010–9019.

[8] J. Lee, D. Jung, J. Yim, S. Yoon, Confidence score for source-free unsupervised domain adaptation, in: International Conference on Machine Learning, PMLR, 2022, pp. 12365–12377.

[9] J. N. Kundu, A. R. Kulkarni, S. Bhambri, D. Mehta, S. A. Kulkarni, V. Jampani, V. B. Radhakrishnan, Balancing discriminability and transferability for source-free domain adaptation, in: International Conference on Machine Learning, PMLR, 2022, pp. 11710–11728.

[10] J. Liang, D. Hu, J. Feng, Domain adaptation with auxiliary target domain-oriented classifier, in: Proceedings of the IEEE/CVF Conference on Computer Vision and Pattern Recognition, 2021, pp. 16632–16642.

[11] F. Wang, Z. Han, Y. Gong, Y. Yin, Exploring domain-invariant parameters for source free domain adaptation, in: Proceedings of the IEEE/CVF Conference on Computer Vision and Pattern Recognition, 2022, pp. 7151–7160.

[12] K. You, M. Long, Z. Cao, J. Wang, M. I. Jordan, Universal domain adaptation, in: Proceedings of the IEEE/CVF Conference on Computer Vision and Pattern Recognition, 2019, pp. 2720–2729.

[13] J. N. Kundu, N. Venkat, R. V. Babu, et al., Universal source-free domain adaptation, in: Proceedings of the IEEE/CVF Conference on Computer Vision and Pattern Recognition, 2020, pp. 4544–4553.

[14] K. He, H. Fan, Y. Wu, S. Xie, R. Girshick, Momentum contrast for unsupervised visual representation learning, in: Proceedings of the IEEE/CVF conference on computer vision and pattern recognition, 2020, pp. 9729–9738.

[15] A. v. d. Oord, Y. Li, O. Vinyals, Representation learning with contrastive predictive coding, arXiv preprint arXiv:1807.03748 (2018).

[16] Y. Kalantidis, M. B. Sariyildiz, N. Pion, P. Weinzaepfel, D. Larlus, Hard negative mixing for contrastive learning, Advances in Neural Information Processing Systems 33 (2020) 21798–21809.

[17] J. Mitrovic, B. McWilliams, M. Rey, Less can be more in contrastive learning, in: Proceedings on "I Can't Believe It's Not Better!" at NeurIPS Workshops, Vol. 137, 2020, pp. 70–75.

[18] C.-H. Yeh, C.-Y. Hong, Y.-C. Hsu, T.-L. Liu, Y. Chen, Y. LeCun, Decoupled contrastive learning, in: European Conference on Computer Vision, Springer, 2022, pp. 668–684.

[19] S. Yang, J. van de Weijer, L. Herranz, S. Jui, et al., Exploiting the intrinsic neighborhood structure for source-free domain adaptation, Advances in Neural Information Processing Systems 34 (2021) 29393–29405.

[20] K. Saito, S. Yamamoto, Y. Ushiku, T. Harada, Open set domain adaptation by backpropagation, in: Proceedings of the European Conference on Computer Vision, 2018, pp. 153–168.

[21] Z. Cao, K. You, M. Long, J. Wang, Q. Yang, Learning to transfer examples for partial domain adaptation, in: Proceedings of the IEEE/CVF

Conference on Computer Vision and Pattern Recognition, 2019, pp. 2985–2994.

- [22] H. Zhao, R. T. Des Combes, K. Zhang, G. Gordon, On learning invariant representations for domain adaptation, in: International Conference on Machine Learning, 2019, pp. 7523–7532.
- [23] L. Du, J. Tan, H. Yang, J. Feng, X. Xue, Q. Zheng, X. Ye, X. Zhang, Ssf-dan: Separated semantic feature based domain adaptation network for semantic segmentation, in: Proceedings of the IEEE/CVF International Conference on Computer Vision, 2019, pp. 982–991.
- [24] S. Li, S. Song, G. Huang, Z. Ding, C. Wu, Domain invariant and class discriminative feature learning for visual domain adaptation, *IEEE Transactions on Image Processing* 27 (9) (2018) 4260–4273.
- [25] Y. Ganin, E. Ustinova, H. Ajakan, P. Germain, H. Larochelle, F. Laviolette, M. Marchand, V. Lempitsky, Domain-adversarial training of neural networks, *The journal of machine learning research* 17 (1) (2016) 2096–2030.
- [26] M. Long, Z. Cao, J. Wang, M. I. Jordan, Conditional adversarial domain adaptation, *Advances in neural information processing systems* 31 (2018).
- [27] S. Cui, S. Wang, J. Zhuo, C. Su, Q. Huang, Q. Tian, Gradually vanishing bridge for adversarial domain adaptation, in: Proceedings of the IEEE/CVF Conference on Computer Vision and Pattern Recognition, 2020, pp. 12455–12464.
- [28] E. Tzeng, J. Hoffman, K. Saenko, T. Darrell, Adversarial discriminative domain adaptation, in: Proceedings of the IEEE Conference on Computer Vision and Pattern Recognition, 2017, pp. 7167–7176.
- [29] S. Cicek, S. Soatto, Unsupervised domain adaptation via regularized conditional alignment, in: Proceedings of the IEEE/CVF International Conference on Computer Vision, 2019, pp. 1416–1425.
- [30] Y. Zhang, B. Deng, H. Tang, L. Zhang, K. Jia, Unsupervised multi-class domain adaptation: Theory, algorithms, and practice, *IEEE Transactions on Pattern Analysis and Machine Intelligence* 44 (5) (2020) 2775–2792.
- [31] V. Prabhu, S. Khare, D. Kartik, J. Hoffman, Sentry: Selective entropy optimization via committee consistency for unsupervised domain adaptation, in: Proceedings of the IEEE/CVF International Conference on Computer Vision, 2021, pp. 8558–8567.
- [32] H. Tang, K. Chen, K. Jia, Unsupervised domain adaptation via structurally regularized deep clustering, in: Proceedings of the IEEE/CVF Conference on Computer Vision and Pattern Recognition, 2020, pp. 8725–8735.
- [33] Z. Deng, Y. Luo, J. Zhu, Cluster alignment with a teacher for unsupervised domain adaptation, in: Proceedings of the IEEE/CVF International Conference on Computer Vision, 2019, pp. 9944–9953.
- [34] Y. Kim, D. Cho, K. Han, P. Panda, S. Hong, Domain adaptation without source data, *IEEE Transactions on Artificial Intelligence* 2 (6) (2021) 508–518.
- [35] S. M. Ahmed, D. S. Raychaudhuri, S. Paul, S. Oymak, A. K. Roy-Chowdhury, Unsupervised multi-source domain adaptation without access to source data, in: Proceedings of the IEEE/CVF Conference on Computer Vision and Pattern Recognition, 2021, pp. 10103–10112.
- [36] X. Su, Y. Zhao, S. Bethard, A comparison of strategies for source-free domain adaptation, in: Proceedings of the 60th Annual Meeting of the Association for Computational Linguistics, 2022, pp. 8352–8367.
- [37] V. K. Kurmi, V. K. Subramanian, V. P. Namboodiri, Domain impression: A source data free domain adaptation method, in: Proceedings of the IEEE/CVF Winter Conference on Applications of Computer Vision, 2021, pp. 615–625.
- [38] J. Liang, D. Hu, J. Feng, Do we really need to access the source data? source hypothesis transfer for unsupervised domain adaptation, in: International Conference on Machine Learning, 2020, pp. 6028–6039.
- [39] V. Kumar, R. Lal, H. Patil, A. Chakraborty, Commix for source-free single and multi-target domain adaptation, in: Proceedings of the IEEE/CVF Winter Conference on Applications of Computer Vision, 2023, pp. 4178–4188.
- [40] J. Dong, Z. Fang, A. Liu, G. Sun, T. Liu, Confident anchor-induced multi-source free domain adaptation, *Advances in Neural Information*

Processing Systems 34 (2021) 2848–2860.

- [41] M. Gutmann, A. Hyvärinen, Noise-contrastive estimation: A new estimation principle for unnormalized statistical models, in: Proceedings of the thirteenth international conference on artificial intelligence and statistics, 2010, pp. 297–304.
- [42] M. Ye, X. Zhang, P. C. Yuen, S.-F. Chang, Unsupervised embedding learning via invariant and spreading instance feature, in: Proceedings of the IEEE/CVF Conference on Computer Vision and Pattern Recognition, 2019, pp. 6210–6219.
- [43] T. Chen, S. Kornblith, M. Norouzi, G. Hinton, A simple framework for contrastive learning of visual representations, in: International conference on machine learning, 2020, pp. 1597–1607.
- [44] Y. Tian, D. Krishnan, P. Isola, Contrastive multiview coding, in: European Conference on Computer Vision, 2020, pp. 776–794.
- [45] D. Dwibedi, Y. Aytar, J. Tompson, P. Sermanet, A. Zisserman, With a little help from my friends: Nearest-neighbor contrastive learning of visual representations, in: Proceedings of the IEEE/CVF International Conference on Computer Vision, 2021, pp. 9588–9597.
- [46] G. Kang, L. Jiang, Y. Wei, Y. Yang, A. Hauptmann, Contrastive adaptation network for single- and multi-source domain adaptation, *IEEE Transactions on Pattern Analysis and Machine Intelligence* 44 (4) (2022) 1793–1804. doi:10.1109/TPAMI.2020.3029948.
- [47] K. Shen, R. M. Jones, A. Kumar, S. M. Xie, J. Z. Haochen, T. Ma, P. Liang, Connect, not collapse: Explaining contrastive learning for unsupervised domain adaptation, in: Proceedings of the 39th International Conference on Machine Learning, Vol. 162, 2022, pp. 19847–19878.
- [48] A. Singh, Cld: Contrastive learning for semi-supervised domain adaptation, *Advances in Neural Information Processing Systems* 34 (2021) 5089–5101.
- [49] M. Thota, G. Leontidis, Contrastive domain adaptation, in: Proceedings of the IEEE/CVF Conference on Computer Vision and Pattern Recognition Workshops, 2021, pp. 2209–2218.
- [50] J. Huang, D. Guan, A. Xiao, S. Lu, Model adaptation: Historical contrastive learning for unsupervised domain adaptation without source data, *Advances in Neural Information Processing Systems* 34 (2021) 3635–3649.
- [51] G. Kang, L. Jiang, Y. Yang, A. G. Hauptmann, Contrastive adaptation network for unsupervised domain adaptation, in: Proceedings of the IEEE/CVF Conference on Computer Vision and Pattern Recognition, 2019, pp. 4893–4902.
- [52] A. Gretton, K. M. Borgwardt, M. J. Rasch, B. Schölkopf, A. Smola, A kernel two-sample test, *The Journal of Machine Learning Research* 13 (1) (2012) 723–773.
- [53] Z. Zhong, E. Fini, S. Roy, Z. Luo, E. Ricci, N. Sebe, Neighborhood contrastive learning for novel class discovery, in: Proceedings of the IEEE/CVF Conference on Computer Vision and Pattern Recognition, 2021, pp. 10867–10875.
- [54] K. He, X. Zhang, S. Ren, J. Sun, Deep residual learning for image recognition, in: Proceedings of the IEEE Conference on Computer Vision and Pattern Recognition, 2016, pp. 770–778.
- [55] C.-Y. Chuang, J. Robinson, Y.-C. Lin, A. Torralba, S. Jegelka, Debiased contrastive learning, *Advances in neural information processing systems* 33 (2020) 8765–8775.